ISTFA™ 2009, Conference Proceedings from the
35th International Symposium for Testing and Failure Analysis
November 15–19, 2009, San Jose, California, USA, p 6-15

Copyright © 2009 ASM International®
All rights reserved.
www.asminternational.org

Gradient Thermal Analysis by Induced Stimulus

Jim Colvin
FA Instruments, Inc.
2381 Zanker Rd. #150
San Jose, CA 95131
(408) 428-9353
E-mail: jim@fainstruments.com

Abstract

In the field of failure analysis of integrated circuits, diagnosing functional failures is a requirement. Traditional beam-based analysis techniques use a scanning laser or e-beam to induce a parametric shift, which is monitored through changes in current or voltage driven to the device. Deep submicron technologies frustrate these analytical methods due to the nearly immeasurable parametric shifts externally caused by a small signal leakage path internally. These internal failures can be identified functionally by timing, temperature or voltage dependencies but the exact location of the fault is difficult to isolate. SIFT (Stimulus Induced Fault Test), RIL (Resistive Interconnect Localization) and SDL (Soft Defect Localization) can identify anomalies functionally using induced thermal gradients to the metal but does not address how to analyze embedded temperature sensitive defects inaccessible to the laser.[1,2,3,4] Stacked die and similar 3 dimensional (3D) devices complicate the analysis requiring destruction/removal of one or more die. This paper will show how to create quantifiable thermal gradients to a defect and triangulate the location of the defect in 1, 2, and 3 dimensions as follows:

1. Apply a differential temperature gradient across the device in each of the X,Y, and Z-axes. The defect is localized based on its measured response in the gradient as the gradient sweeps across.
2. Induce a gradient with a laser and use the measurement of DC power required to relate the distance to the defect from various locations in relation to a heat sink.
3. Measure the time of flight of the thermal propagation to a defect from known laser positions to triangulate the location of the defect.

Introduction

The Stimulus Induced Fault Test (SIFT) system is the basis for Time of Flight (TOFSIFT) and thermal gradient development.[5] Since the SIFT scanner does not use traditional laser scanning microscope optics, the Device Under Test (DUT) scan area can be submicron to 12" or more, allowing whole boards, packages and die to be analyzed since the scanners are stepper-based rather than internal optics based. Field of view limitations of objectives on LSM (Laser Scan Microscope) based equipment are eliminated with SIFT. Data output is to a PC via the microcontroller and contains data from the scan for X, Y, Z and multi-channel data for each step in the scan. This data is coordinate data but can also be displayed photographically. Channel data consists of pass/fail signals from the tester as well as analog information. The scan and step is user defined based on spot size.

Unlike LSMs, SIFT uses a stationary beam and moves either the stage or the microscope head in a raster scan pattern. Figure 1 is a block diagram of the apparatus. A microscope and stage are equipped with stepper motors to control the X, Y, and Z motion of the scan. Z control is necessary to control the spot size of the stimulus by either focus or proximity control of the source. Laser based SIFT uses a laser attached to the top camera port of the microscope and can be any wavelength compatible with the selected optics. The selected objective, aperture, and focus control spot size, in this case.

High power solid state or CO_2 lasers are mounted in place of the microscope and raster scanned over large areas for thermal and TOFSIFT. The stimulus can also be introduced over the DUT with the raster applied to the stage. This method of SIFT can be thought of in the same way a probe is positioned over a DUT by moving the stage. The added requirement for TOFSIFT is the ability to position the laser at predetermined locations and modulate/raster the laser to determine the length of time the defect "responds" to the thermal wave and the corresponding length of time for the defect to cool. These time measurements are obtained at multiple locations to triangulate in 3D the location of the defect akin to Global Positioning System (GPS) trilateration methods.[6,7]

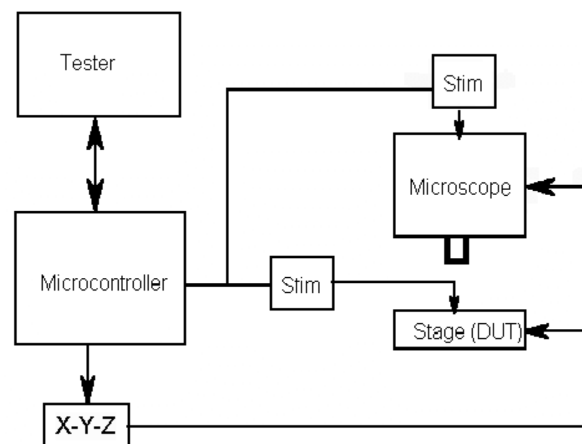

Figure 1. Block Diagram of SIFT Scanner.

Differential TLS Methods

Differential TLS builds the foundation for TOFSIFT and in its own right simplifies the task of isolating the regions of interest. Figure 2 is a curve showing an unexpected jump in Idd at 10 volts. The hysteresis moves to lower voltages at elevated temperatures with minimal change in Idd. Two SIFT scans at 1428nm were performed thermally similar to TIVA/OBIRCH methods at 8 volts, for the lower and upper portions of the loop. The 2 scans were overlaid in green and red with blue as the background. Figure 3 shows the differential areas in either green or red, with all yellow regions indicative of a common mode response. Unfortunately this data does not clearly show which areas stimulated by the laser improve or degrade the hysteresis loop.

Since the laser coordinates are known, the laser can be steered to and parked on each of the regions of interest maintaining constant power and focus. Two related nodes are isolated in figure 4 responsible for the threshold shift. This example illustrates the false positives created when a focused laser is used to scan across the die. Gradient SIFT and TOFSIFT avoid these situations since the temperature differential is not severely localized.

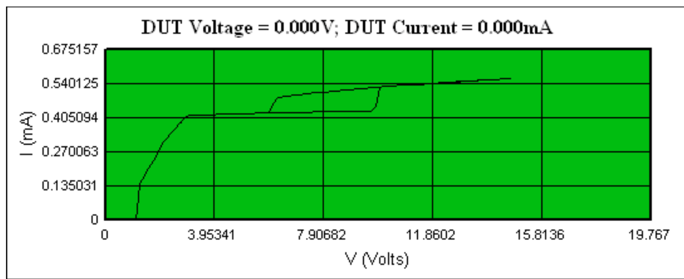

Figure 2. Idd curve showing unexpected hysteresis activating at 10 Volts and relaxing at 6 volts.

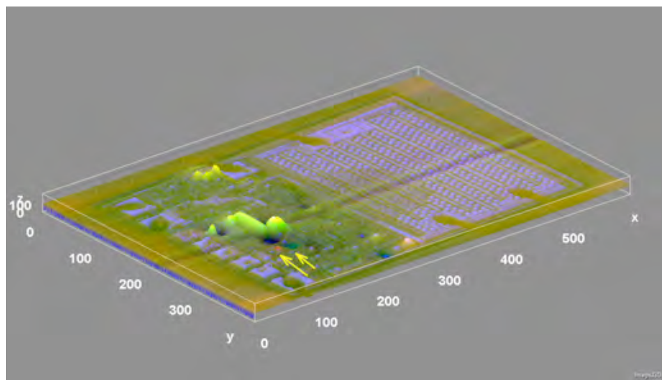

Figure 3. SIFT TLS scan of differential bandgap shift. Green and Red areas (arrows) show regions of shift associated with the hysteresis loop.

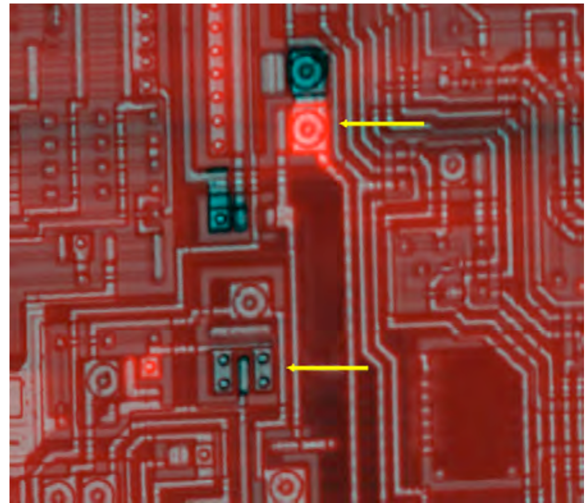

Figure 4. Locations responsible for shifting the hysteresis to lower voltages from figure 3.

Thermal Stimulus

Parametric issues surrounding thermal management need to be understood so that appropriate power levels can be chosen for both frontside as well as backside analysis. A simple way to determine the required energy is to look at a diode to substrate on the device under test. Generically, the substrate diode associated with a given input pin is a known temperature sensor. Figure 5 shows the change in forward voltage for 0.1mA, 1mA, and 2mA respectively.

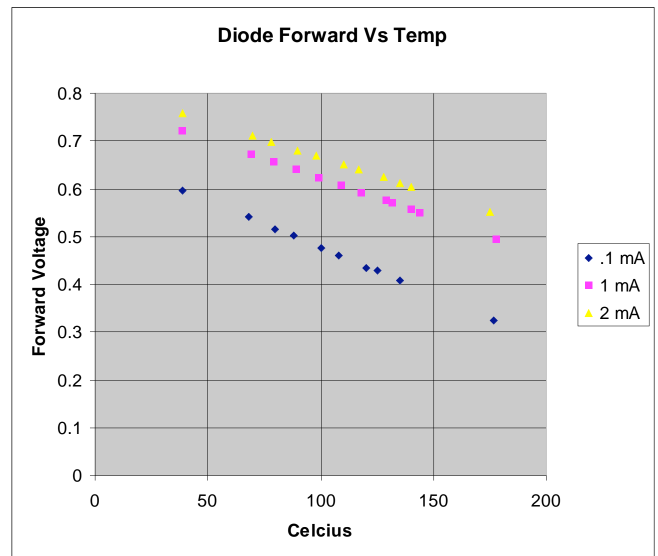

Figure 5. Typical diode forward drop versus temperature relationships for 3 current drive levels.

Whereas the forward voltage may vary process to process, the ΔV can still be used to measure temperature excursions as shown in equation 1.

Equation [1]

$$\Delta V/2.0E\text{-}3 \cong \Delta T \quad @0.1mA$$
$$\Delta V/1.6E\text{-}3 \cong \Delta T \quad @1mA$$
$$\Delta V/1.5E\text{-}3 \cong \Delta T \quad @2mA$$

ΔV = Change in diode forward voltage
ΔT = Celsius change in temperature

The next parameter to evaluate is the thermal propagation in silicon for frontside and backside. For frontside, the excursion in temperature is fairly small, on the order of 5 to 10 degrees, as shown in Figure 6. Note the small fast waves are the on-off pulses of the laser and the general slope downward represents general die heating. Since the substrate is tied to a copper paddle, the general die heating is reliant on the paddle, which is floating. The temperature gradient is only 4 to 5 degrees Centigrade due to the thermal conduction of the die and paddle.

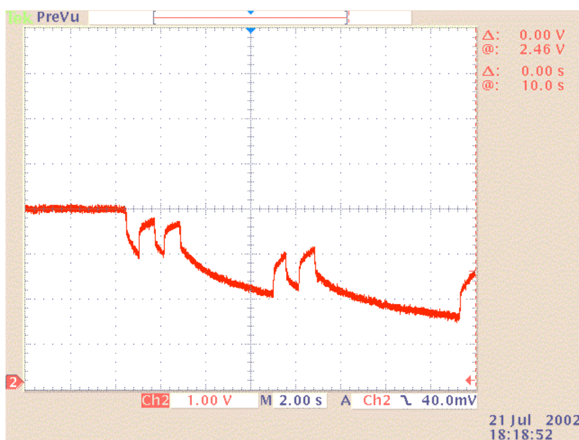

Figure 6. Thermal excursions with a pulsed IR laser on the frontside of silicon. Signal is inverted. Scale is Horz.: 2 sec./div., Vert.: 5^0 C/div.

For the backside, a die was thinned to 30 um remaining silicon thickness in order to evaluate lateral heat spread with very thin substrates. Lateral effect vs. thickness and resolution will be discussed in applicable sections later in the paper. Note the rapid ramp and gradient now better than 100 ^{0}C. Since the silicon is thin and has greatly reduced volume there is much less lateral heat spread and a high differential thermal gradient.

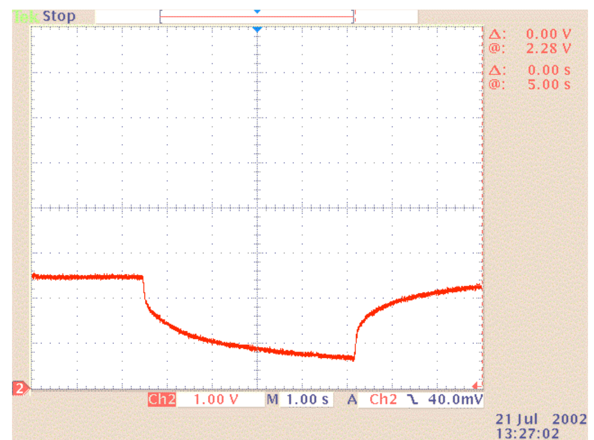

Figure 7. Thermal excursions with a pulsed IR laser on the backside of silicon. 30um thickness. Signal is inverted. Scale is Horz.: 1 sec./div,Vert.:100 ^{0}C/div.

Thermal Stimulus using CW lasers

Normally for thermal stimulus with a laser, wavelengths outside the indirect bandgap of silicon are required, such as 1.3 um, to avoid generation of photocurrents.[1,4] It is difficult to get the power necessary in a large spot to heat significantly at this wavelength due to numerous factors such as laser power limitations. The silicon doesn't heat at this wavelength. The primary heating is accomplished from absorption of the laser energy by the metal, which typically scatters a significant amount of the radiation. As reported by Cole et al, the temperature gradient at metal is roughly 1^0C/mW with typical heating of the metal up to around 30^0C with a 1.3 um laser.[1] Temperature excursion of the related silicon will be typically less than 1^0C, inadequate for silicon based thermal analyses.

Ordinarily, shorter wavelength lasers generate too much photocurrent to be useful thermally. Several laser wavelengths of importance, due to their ability to generate higher power, are: 532nm, 808nm, 940nm, and 1064nm. All of these wavelengths will generate photocurrents unless they are masked from the die. This is accomplished by applying high temperature flat black paint to the die surface by spray, brush or spin deposition. The 532nm laser does not typically need to be masked when used backside due to the absorption of the laser by the silicon substrate. Carbon sputtering or carbon paint (preferred) can also be used backside or frontside if the connections are passivated . A 5 watt 808nm laser was chosen to locally heat the surface with around 1 to 2 watts depending on spot size and desired heating for the above work. For the remainder of the paper, a CO_2 laser will be used.

Gradient Thermal Analysis

A straightforward method to localize a thermally sensitive region either parametrically or functionally is possible when opposing ends of a copper paddle are held at two different temperatures. A corresponding precise thermal gradient will form across the surface. With a quantifiable temperature gradient across the device in X, Y, and optionally Z; the location of the defect can be better localized. Similar to

Magnetic Resonance Imaging except that the field gradient is replaced with a thermal gradient and the defect is the detector.[8] Two precision temperature controllers are required to control and "walk" the gradient across the wafer as shown in figures 8 and 9. The greater the gradient and the tighter the tolerance of the defect to temperature change, the better the triangulation of the defect. The technique assumes the defects are not distributed, however a cluster can still be localized. Once the X position is approximately obtained with a low level gradient, the differential is increased to more precisely localize the defect while avoiding the continuity issues that walking extreme differential temperatures across the wafer create. The wafer or Peltier elements are repositioned 90 degrees in order to localize the Y direction. Since the technique is effectively static, the test time is irrelevant. Loop testing or 1 shot testing can be performed for pass/fail with a gradient scan or binary search for the threshold temperature at which the gradient is locally at the fail temperature in conjunction with the defect. The probe card can be easily positioned over the differential heating system. Wafers that dissipate heat while tested can still be analyzed, however, the thermal offset will need to be factored into the gradient measurements and/or a burst mode test will need to be performed in order to minimize unwanted substrate heating. Forcing a gradient across a thick metal plate of which the wafer is attached and using closed loop control on the ends is the best method to minimize these issues but takes significantly more power from the controllers if large gradients are desired. Heat load of the Peltier needs to be considered for long term dissipation into the wafer chuck. A high power temperature controlled chuck capable of cooling serves well to obviate these issues. Although 2 Peltier units are shown here, a chuck could be used to control the cold side of the gradient with a Peltier, liquid or resistive heater forcing the other side.

Referring to equation 2, precision control of the gradient means obtaining the best triangulation data in conjunction with the minimum temperature change required to detect the defect.

Equation [2]
Resolution=Gradient*Precision/ΔChange

If the minimum temperature change required to see a transition from pass to fail ranges from 40.1^0C to 40.2^0C, then the defect will be resolved (Precision/ΔChange) within a gradient of 0.1^0C. These assumptions are based on precise temperature control and a single defect. A chosen gradient of 1^0C/mm will yield a best-case resolution of 100um in X and Y. Correspondingly, the measurement precision of leakage as a function of temperature and the slope of the induced gradient define resolution. If a device is characterized with a defect which changes by 1 ohm/^{0}C and the precision of the measurement is 0.01 ohms then the thermal gradient inside 0.01^0C is within the range of error. A gradient of 1000um/^{0}C will then infer the triangulation is within 10um in X and Y.

In order to minimize the impact of changing temperatures with a sweeping thermal gradient, the defect can be characterized with a few precise data points at various temperatures resulting in a best fit line or curve applied to the data. A static gradient is then applied and the measured leakage matched to the point on the curve.

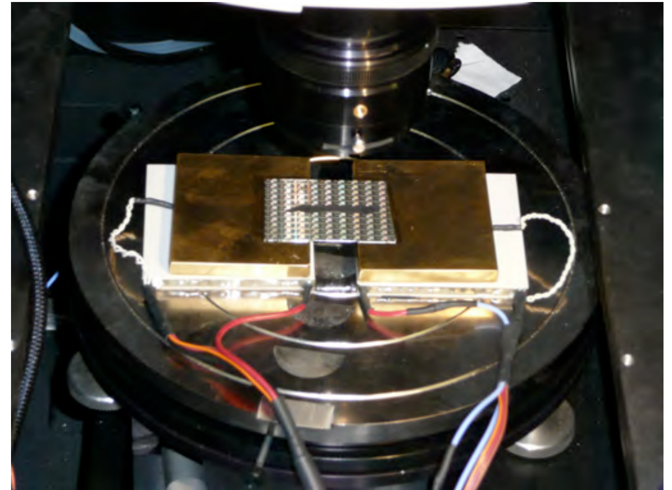

Fig 8. Wafer section across 2 Peltier temperature controlled plates for differential temperature control. The wafer was thermally coupled using mineral oil for the experimental data. Local vacuum on each brass plate may also be used to hold the wafer edges.

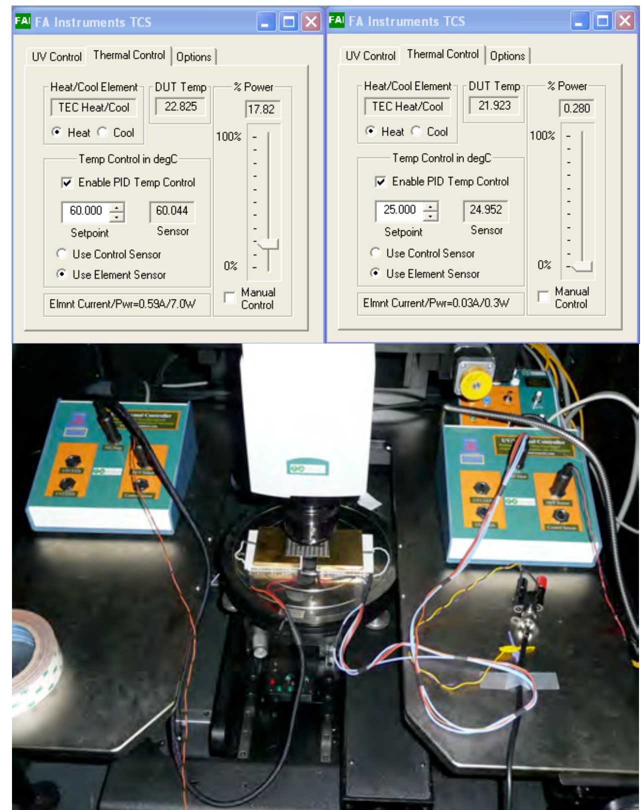

Figure 9. Differential temperature control panels (upper image) and the controllers (lower image). Each panel can control the forcing temperature, quickly within 50 mK.

Infrared investigation with an InSb camera as seen in figure 10 was used to measure the quality of the gradient generated across the wafer. Carbon paint was used to calibrate out issues with black body radiation and pixel registration errors during measurement.

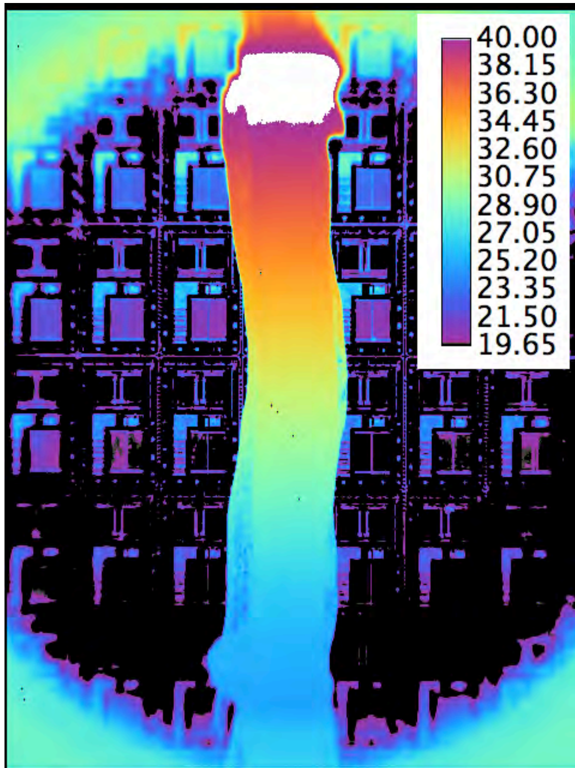

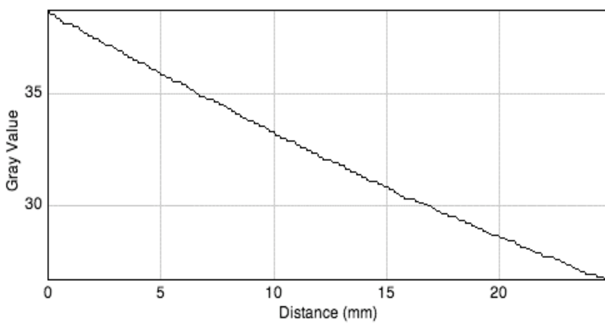

Fig 10. 350um thick wafer section with induced thermal gradient. Temperature gradient is 15^0C across a 25mm gap. Carbon paint was used to validate the gradient while imaged with an InSb thermal camera. This step was only used to validate the gradient data and is not necessary for the actual work.

Package devices are more problematic due to the differing materials and hence thermal conductivities. Additionally, the socket fixturing must be customized with direct contact made to the edges of the internal copper paddle of the device in order to induce a decent thermal gradient. Figures 12 through 14 illustrate the problem. The package was backside milled and the die thinned as in normal backside practice to 75um. The reason for thinning was to better match the thermal gradient of the plastic to that of the die since a thin die has less lateral conduction. Unfortunately, for a 15^0C spread across the package the expected gradient across the die portion was anticipated to be not much less than 12^0C and was found to actually be 1^0C. This method therefore requires direct thermal connection to the conductive substrate or paddle using machined fingers to make contact. Package sockets can be incorporated with this, especially in the case of flip chip or bump chip technologies where either the back face is perfectly accessible or a large area heat sink can be induced with a thermal gradient in the case of power processors.

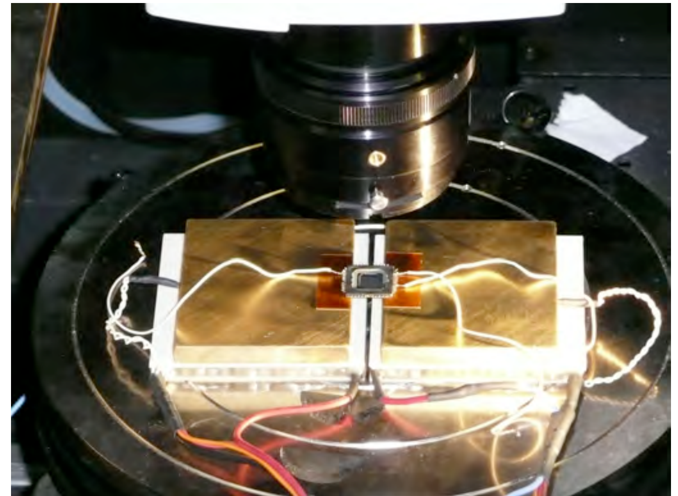

Fig 11. TQFP package across the differential temperature controller. Double sided Kapton tape was used to temporarily attach the package edges to the plates. The die was backside thinned to 75um.

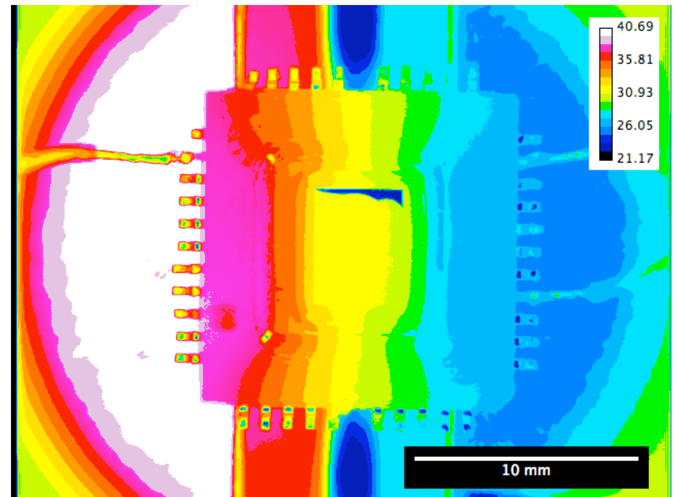

Figure12. InSb thermal image of the gradient across the package. Note the package has larger temperature steps while the die has smaller steps.

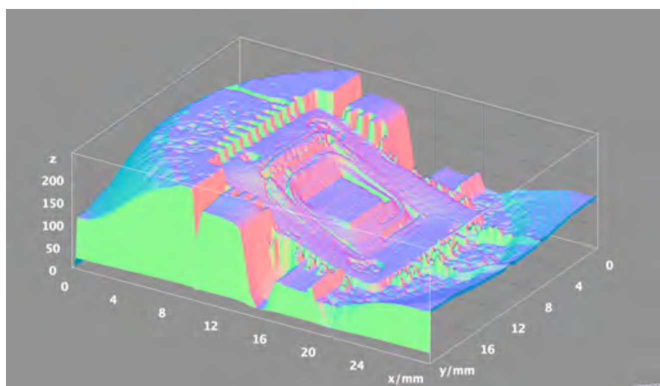

Figure 13. 3D profile of figure 12 above. The profile shows even with the thinned die at 75 um, the silicon develops a small gradient in relation to the package.

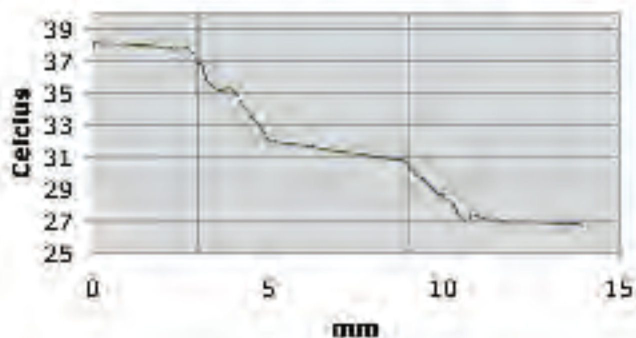

Figure14 Line profile from figure 13. The slope illustrates a 1^0C gradient on the silicon in spite of a 12^0C gradient across the package in that region.

Laser Induced Gradient Thermal Analysis

The thermal laser can be used in place of one of the 2 Peltier controllers or opposite a heat sink where package complexities obviate access. A thin slot can be milled along the package edge on angle to allow access with the laser to the die edge. Carbon paint can be used to assist laser absorption as long as the die edge has no delamination issues to allow the carbon paint to wick into sensitive areas. The laser serves as the heat source vs. the heat sink. The steady state power required to reach the transition threshold is noted at known locations. A line scan can be used to uniformly inject higher levels of average power along an entire edge to maintain and "walk" the gradient across the region of interest. The power required is recorded preferably for each of the 4 edges or at select points appropriate to the geometry of the bulk region. This method allows the measured power of the laser required to reach the trip point or threshold associated with the failure to be related to the distance to the defect. Select input pins should be used for temperature calibration and validation of the linearity of the gradient across the die. Nonlinear effects can be mathematically line fitted by utilizing the multiple pad diodes available on the device before actual testing begins. Optimization of the above techniques can be accomplished by restricting the gap the gradient is applied. The gradient can, therefore, be large while avoiding excessive temperatures at the edges.

Time of Flight Thermal Analysis (TOFSIFT)

All of the prior methods require a heat sink and source in order to create the thermal gradient. In the case of 3D structures such as stacked die technologies, it is difficult to contact the edges of the die since the individual die are typically of differing dimensions. The apparatus for TOFSIFT (Time of Flight Stimulus Induced Fault Test) consists of a thermal laser, a programmable fast A/D or comparator to detect the threshold from the part either as pass fail data or analog change and the ability to control the hysteresis of the on to off threshold point at which the laser is fired. The laser power is controllable for both the on power and the off power states. (Typically the off power is 0). The local heating of the device is controlled by the dwell time of the laser required to trip from pass to fail. Averaging for a matrix of locations results in improved triangulation.

For this emerging technology, a 10 um CO_2 laser was chosen in order to heat a controlled spot with a diameter down to 100um. The diameter of the spot is less important than the damage threshold. Accurate placement of the spot is key since the triangulation is determined proportionately by the ratio of the radius. Identification of the locus or intercept of the corresponding radii can be scaled proportionately to match the physical distance even if the speed of the traveling thermal wave is unknown. The ratio of the TOF between known coordinates to the defect is scaled to best fit the locus in the case where measuring the TOF is impractical. The spot needs to be large enough to heat the die without local damage. If the laser modifies the surface, the black body radiation absorption will change affecting the measurements. The power used was 1 to 1.5 Watts with a 0.5mm dia spot. The laser range is from 100mW to 10 Watts and for larger spot sizes in pulse mode the higher powers are indeed used.

Parametric issues surrounding thermal management need to be understood so that appropriate power levels can be chosen for both frontside as well as backside analysis. A simple way to determine the required energy is to look at a diode to substrate on the device under test as explained above. Generically, the substrate diode associated with a given input pin is a temperature sensor, which can be calibrated. Figures 15 and 16 show the response of two input pins on opposite sides of a 5mm die. The hysteresis of the trip point to turn the laser on and off is determined experimentally. If the trip points are too close together, the laser can fire prematurely. Ideally, the on to off states should be chosen at around a 50% duty cycle upon setup at the first laser injection site. The cooling of the die and heating by laser normalize out die temperature issues and allow the die to act as a thermally stimulated oscillator. The frequency of the oscillator changes in proportion to the distance of the injection point to the defect or bond pad diode monitor. Candidates for this technique are devices that exhibit either a repeatable temperature instability or a temperature dependent resistance change. A characterization of the failure first is paramount to understanding the thermal gradient range

and hence laser power/hysteresis settings. The montage in figure 17 is a sequence of thermal images during the on portion of the laser pulse. The thermal propagation from the corner of the square copper paddle is clearly shown. The cycle times were on the order of 500 to 900msec for this particular sample to an input diode chosen as the "defect" hereafter. The sample is a TQFP package 14mmx14mm with an exposed copper paddle from the backside milled using the ASAP-1. The die is 500um thick and the Cu paddle is 250 um thick. The total Z distance to the die face is 750um. Carbon paint was applied to normalize the laser absorption. The laser was programmed for 4 corners of the paddle and the center in micrometers, the results follow:
Site A: (5880,0,0) 680msec. Site B: (0,0,0) 976msec.
Site C: (0,5260,0) 832msec.
Site D: (5880,5260,0) 512msec.
Center Site E: (2940,2630,0) 424msec.
Measured propagation time:895msec/5880um

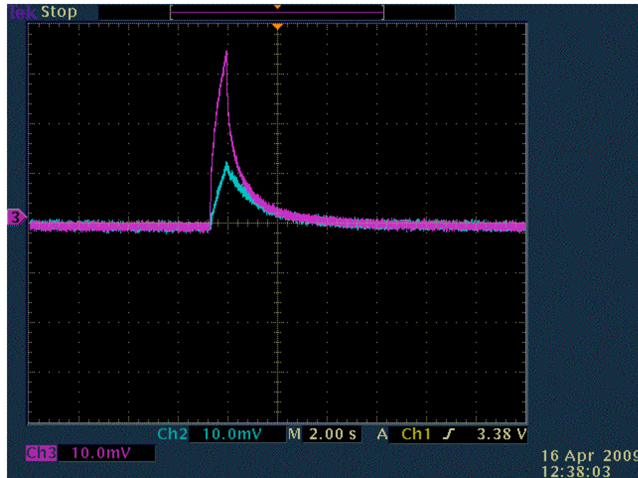

Figure 15. Thermal excursions with a pulsed IR laser on the backside of silicon. 75um thickness. Scale is Horz.: 2 sec./div.,Vert.:1^{0}C/div. A clear difference can be seen between the diodes.

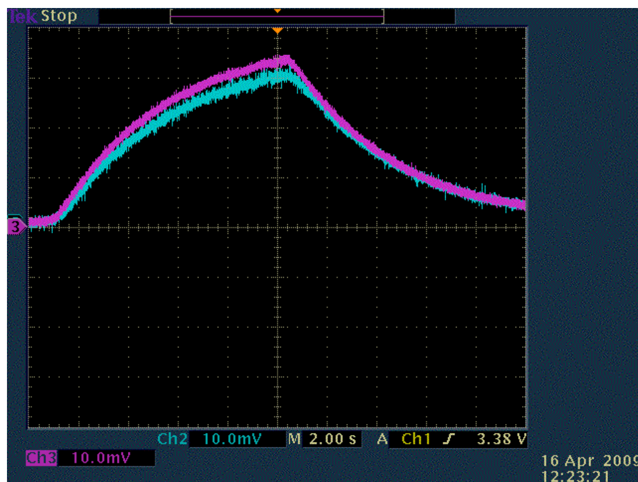

Figure 16. Thermal excursions with a pulsed IR laser on the plastic backside of the intact PQFP package. The low thermal conductivity of the plastic results in an inadequate difference signal for the analysis.
Scale is Horz.: 2 sec./div.,Vert.: 1 ^{0}C/div.

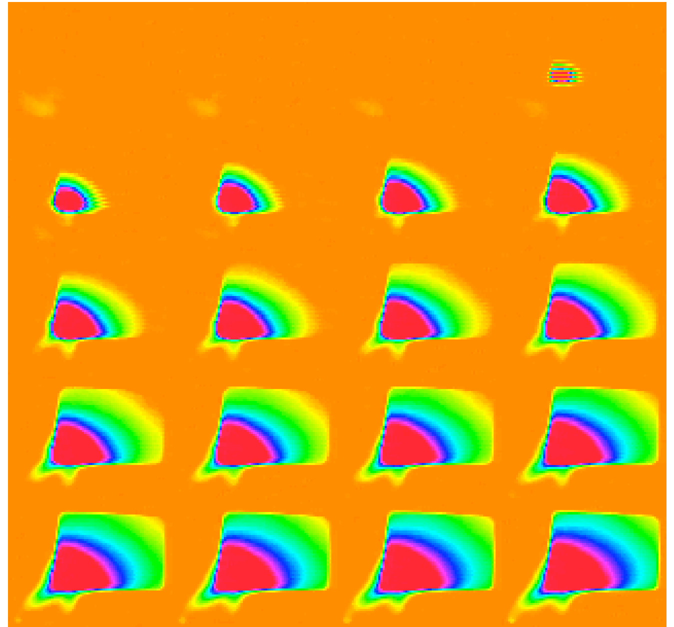

Figure 17. Montage of the thermal wave propagating for one on_cycle from the lower left corner. Each frame is 1/30 sec. taken with an InSb camera. Note the wave front gradient (slope) reduces as it propagates.

All the laser points are in the Z=0 plane. The implications will become clear later in the paper. For now consider the 2 dimensional case. Referring to figure 18, the 3 data points furthest are chosen and overlaid with radial patterns proportional to the measured laser period. From this, the propagation time is determined and the location of the defect is already approximately determined. Triangulation is shown in figures 19 and 20 by using 3 circles and calculating the intercept points per the following formula in Equation [3]:

Equation [3]
$X^2+Y^2=R^2$ (for sites A, B, C)
A-B=B-C (Intercept calculation for 3 circles A, B, C)

Sites D and E overlap the identified location. Site E is in the center and Site D is closest to the defect. The Z plane has been ignored up to this point but D and E have significant Z angle with the opposite side of the triangle in Z at 750um below Z=0. Since the purpose is to triangulate in 3D, the 2D case does a disservice to the acquired data. Using the intercept method is convenient but as shown in figure 20 unwanted measurement error results. Additionally, since the defect is not on the same z=0 plane, error compounds as the slope of the z vector increases.

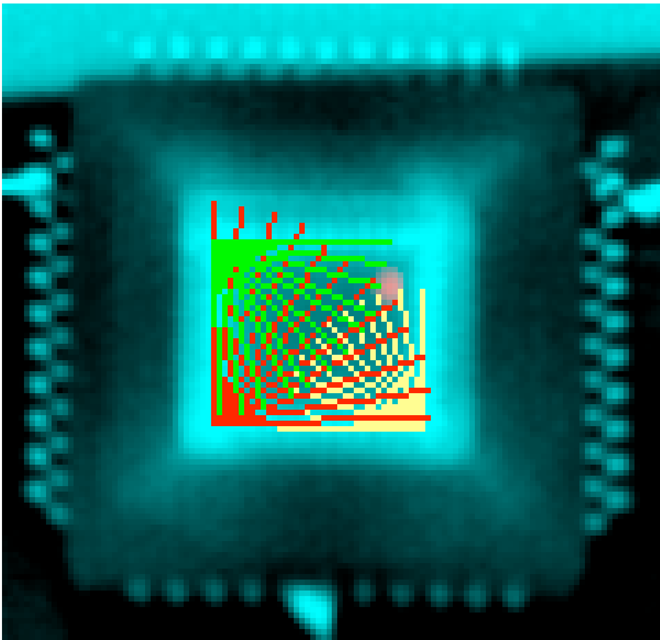

Figure 18. Radial spread patterns illustrating the propagation of the thermal wave from 3 corners of the copper paddle in a PQFP package accessed from the backside. The actual fail location is at the conjunction of the 3 arcs and is an emission overlay aligned from an equivalent part to validate the technique. A CO_2 laser was pulsed to induce the thermal wave in conjunction with a feedback loop.

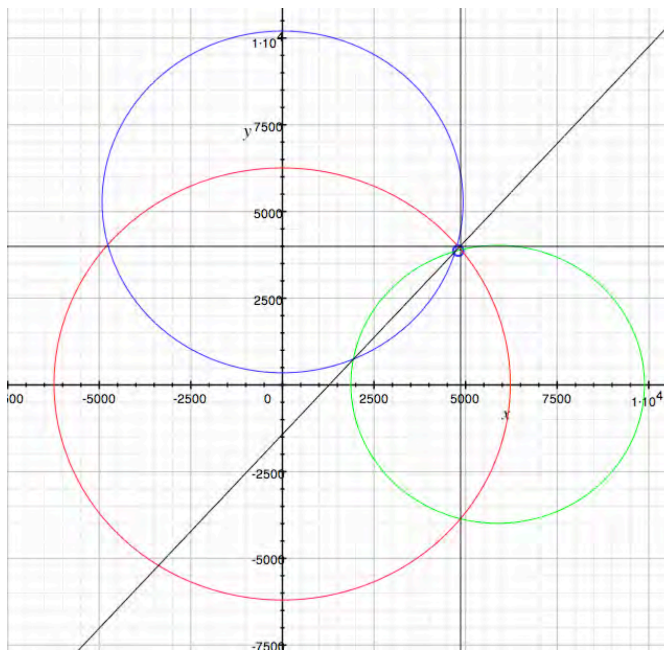

Figure 19. Triangulation in microns of the 3 thermal injection points to the identified locus in 2D from figure 18 above using intercepts. The distant points must be used to minimize Z error.

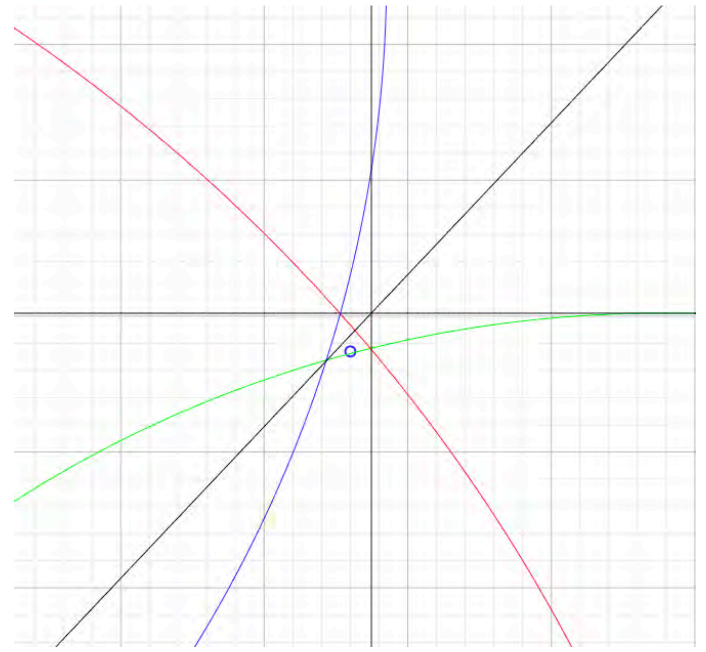

Figure 20. Zoom view of the locus from figure 19 illustrating the resultant error with the intercept.

Plotting the 3D case clarifies the remaining 2 issues. Equation set 2 is a 3D matrix set for all 5 data points. The propagation period for Z is longer than X-Y due to the die attach. In this case, the copper paddle is heated. The propagation takes 2.5X longer to reach the die through the die attach. The ratio is calculated by the Pythagorean theorem from the center point to the identified locus in order to approximate the hypotenuse length. Applying equation set 4 yields a 3D view of the spherical propagation waves as shown in figure 21. The first 5 equations define the spheres where the center x,y,z location is defined by x_a,y_a,z_a for sphere a through x_e,y_e,z_e for sphere e. The radius of each sphere is the time a_{msec} through e_{msec} divided by the propagation time constant s_{msecum} in milliseconds/micrometer. Variables t and u define the continuous set of points to plot in 3D space defining a portion or the entire sphere surface to be displayed.

Equation set [4]

$$\begin{bmatrix}x\\y\\z\end{bmatrix}=\begin{bmatrix}x_a\\y_a\\z_a\end{bmatrix}+\begin{bmatrix}\sin t\sin u\\\sin t\cos u\\\cos t\end{bmatrix}\left(\frac{a_{msec}}{s_{msecum}}\right), t=0\ldots 2\pi, u=0\ldots 1\pi$$

$$\begin{bmatrix}x\\y\\z\end{bmatrix}=\begin{bmatrix}x_b\\y_b\\z_b\end{bmatrix}+\begin{bmatrix}\sin t\sin u\\\sin t\cos u\\\cos t\end{bmatrix}\left(\frac{b_{msec}}{s_{msecum}}\right), t=0\ldots 2\pi, u=0\ldots 1\pi$$

$$\begin{bmatrix}x\\y\\z\end{bmatrix}=\begin{bmatrix}x_c\\y_c\\z_c\end{bmatrix}+\begin{bmatrix}\sin t\sin u\\\sin t\cos u\\\cos t\end{bmatrix}\left(\frac{c_{msec}}{s_{msecum}}\right), t=0\ldots 2\pi, u=0\ldots 1\pi$$

$$\begin{bmatrix}x\\y\\z\end{bmatrix}=\begin{bmatrix}x_d\\y_d\\z_d\end{bmatrix}+\begin{bmatrix}\sin t\sin u\\\sin t\cos u\\\cos t\end{bmatrix}\left(\frac{d_{msec}}{s_{msecum}}\right), t=0\ldots 2\pi, u=0\ldots 1\pi$$

$$\begin{bmatrix}x\\y\\z\end{bmatrix}=\begin{bmatrix}x_e\\y_e\\z_e\end{bmatrix}+\begin{bmatrix}\sin t\sin u\\\sin t\cos u\\\cos t\end{bmatrix}\left(\frac{e_{msec}}{s_{msecum}}\right), t=0\ldots 2\pi, u=0\ldots 1\pi$$

$$\begin{bmatrix}x\\y\\z\end{bmatrix}=\begin{bmatrix}4800\\3870\\1900\end{bmatrix}=\begin{bmatrix}4800\\3870\\1900\end{bmatrix}$$

$$\begin{bmatrix}x\\y\\z\end{bmatrix}=\begin{bmatrix}4800\\3870\\1900\end{bmatrix}u, u=0\ldots 2$$

Constants:
s_{msecum}=895msec/5880um
a_{msec}=680msec
b_{msec}=976msec
c_{msec}=832msec
d_{msec}=512msec
e_{msec}=424msec
x_a=5880um
y_a=0um
z_a=0um
x_b=0um
y_b=0um
z_b=0um
x_c=0um
y_c=5260um
z_c=0um
x_d=5880um
y_d=5260um
z_d=0um
x_e=2940um
y_e=2630um
z_e=0um

The TOFSIFT method has been successfully used to localize both leakage failures and functional failures. Failures with hysteresis or instability are problematic. Hysteresis failures must be analyzed 1 shot or with a reset to clear the hysteresis for each new measurement cycle. Unstable devices need some repeatability to be analyzed. The severity of the instability dictates the resolution. Errors in the Z model for stacked die have been observed similar to the problem with die attach in figure 21. Different thermal conduction of the die attach requires a compensator (multiplier) to be applied depending on the die stack. Currently, this is determined experimentally by comparing the TOF data from several additional locations roughly equidistant from the approximate location of the defect. Delamination/void issues can be overcome with carefully milled access points along the die edges of the stacked array.

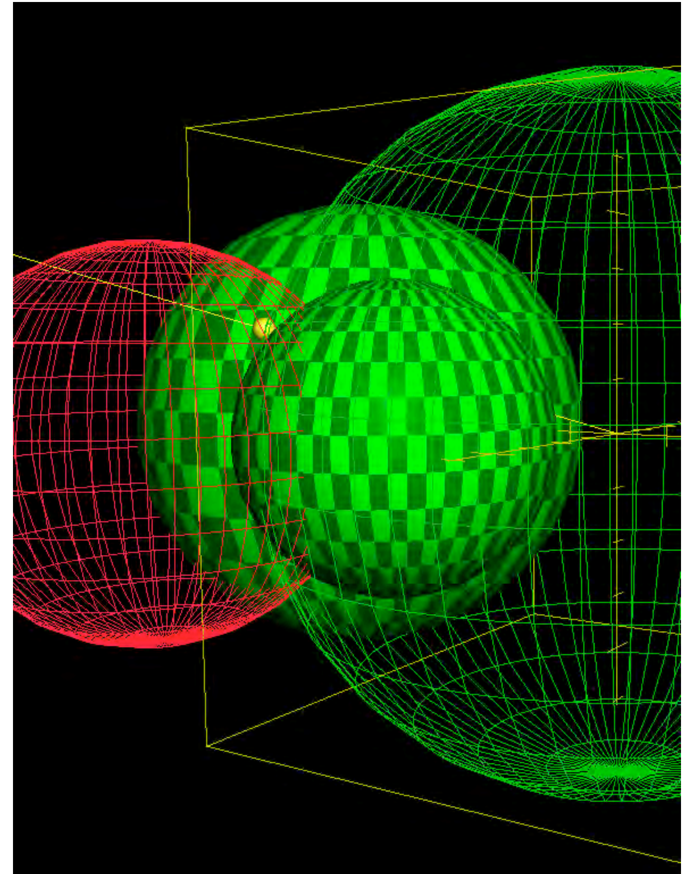

Figure 21. Error from the edge coordinate closest to the defect. The error is caused by the fact that the injection point into the copper paddle is off the edge of the die by approx. 500um. The thermal wave must couple up to the die further from the stimulus laser causing the spherical pattern (red) to appear too large in relation to the yellow dot (defect) at the locus of (4800, 3870, 750).

Ongoing Work

GPS devices calculate position using a technique called "3-D multilateration", which is the process of figuring out where several spheres intersect.[7] In the case of GPS, each sphere has a satellite at its center and for TOFSIFT the laser is at the center; the radius of the sphere is the calculated distance from the laser spot to the defect per equation 5.

Equation [5] $d=\mathrm{sqrt}((x_2-x_1)^2+(y_2-y_1)^2+(z_2-z_1)^2)$

Ideally, these spheres would intersect at exactly one point, with one possible solution to the current location, but in reality, the intersection is a culmination of near proximity surfaces. The defect can be located within any point in the proximal area compounding the error. Precision is said to be "diluted" when the area grows larger, dilution of precision or (DOP) is a measure of the error factor. The same concepts apply to TOFSIFT and as such, strikingly similar algorithms are used to calculate position but on a considerably slower timescale at shorter distances. The process can be automated

to position and fire the laser as well as calculate the locus with averaging to minimize error. The (TOA) Time Of Arrival or (TDOA) Time Difference Of Arrival are two of multiple algorithms available to provide a best-fit solution to multilateration. The chosen CO_2 laser has poor power stability and slow response since it is a gas discharge laser requiring power control through pulse width modulation. Trilateration improvements are being explored for both solid state and gas discharge lasers. Finite element models can be incorporated to improve 3D triangulation in complex packages and used in conjunction with CAD views.

Conclusions

An emerging method of failure analysis has been presented which now allows buried defects to be triangulated using thermal gradients. The gradient is either gradually walked across the die while the device is tested or pulsed to determine the propagation delay time to the defect. Inducing a controlled gradient either static or dynamic across each axis allows the defect distance to be identified and matched to the gradient. Once this is accomplished in X, Y, and Z; the embedded location of the defect is known. Triangulation to 10um has been shown in 2D space with static thermal gradient methods and 100um in 3D space with pulsed time of flight methods. The coordinate data allows localization of failures in stacked die as well as single die for localized small access holes to be milled. Traditional techniques can then be used to triangulate further, if required. This technique works both with traditional parametric measurements as well as thermally sensitive soft defect test failures. Existing input pins are used to assist in calibrating the gradient for triangulation or the data may be scaled for best fit of the trilateration data without benefit of calibration points.

Acknowledgments

To my wife Mayra for her devotion and patience with my continuing to burn the candle at both ends and my son Christopher for helping assemble the video animation files.

References

1. U.S. Patent # 6,078,183 “Thermally-induced voltage alteration for integrated circuit analysis,” Cole, Jr.; Edward I. Sandia Corporation (Albuquerque, NM)

2. Bruce et al., "Soft Defect Localization (SDL) on ICs", Proceedings From the 28th ... Symposium for Testing and Failure Analysis (ISTFA), pp. 21-27, Nov. 3-7, 2002.

3. E.I. Cole, P. Tangyunyong, CF Hawkins, MR Bruce, VJ Bruce, RM Ring, WL Chong “ Resistive Interconnect Localization” ISTFA 2001 pp. 43-50.

4. J. Colvin,”Functional Failure Analysis by Induced Stimulus” ISTFA/2002 Proceedings, pp. 623-630.

5. U.S. Patent # 7323888 B1 “System and Method for Use in Functional Failure Analysis by Induced Stimulus,” Colvin; James B.

6. Ivan Stojmenović,”Handbook of Sensor Networks: Algorithms and Architectures” p. 290. Wiley SBN: 978-0-471-68472-5 Hardcover 552 pages.

7. R. Bucher and D. Misra,” A Synthesizable VHDL Model of the Exact Solution for Three-dimensional Hyperbolic Positioning System” VLSI Design, 2002 Vol. 15 (2), pp. 507–520

8. J. Hornak, ”The Basics of MRI” http://www.cis.rit.edu/htbooks/mri/index.html